Check for updates

Response surface methodology optimization and kinetic study of isobutene/2-butene alkylation reaction

Kaiwei Fu[1] · Xiaopeng Chen[1] · Zhiyu Chen[1] · Chenghong Wu[1] · Xu Wei[1] · Jiezhen Liang[1] · Weijian Nong[2,3] · Linlin Wang[1]

Abstract

The multi-factorial analysis was carried out for the alkylation reaction of isobutene/2-butene with response surface methodology (RSM), and a quadratic model was developed. The reaction conditions optimized by the quadratic model were obtained as follows: reaction time of 7 min, reaction temperature of 5 °C, and stirring speed of 1500 rpm. The relative error between the estimated value (76.72%) and the experimental value (77.47%) of the selectivity of TMPs was 0.98% under such reaction condition. The model well represents the correlation between the selectivity of TMPs with the reaction time, reaction temperature and stirring speed. The kinetic model for the alkylation reaction of isobutene/2-butene was developed according to the classical carbonium ion mechanism, where the catalyst was sulfuric acid. The kinetic parameters were fitted with nonlinear least squares to obtain reasonable rate constants and confidence intervals. The activation energies and pre-exponential factors calculated from the Arrhenius relationships, where the activation energy of the main reaction was 16.03 kJ/mol, and the activation energies of other side reactions ranged from -62.59 to 59.94 kJ/mol.


✉ Linlin Wang
  wanglinlin1971@sina.com

1   Guangxi Key Laboratory of Petrochemical Resources Processing and Process Intensification Technology, School of Chemistry and Chemical Engineering, Guangxi University, Nanning 530004, China

2   China Academy of Science and Technology Development Guangxi Branch, Nanning 530022, China

3   Guangxi Sci-Tech Development Forest-Like Technology Co. LTD, Nanning 530022, China

Graphical abstract
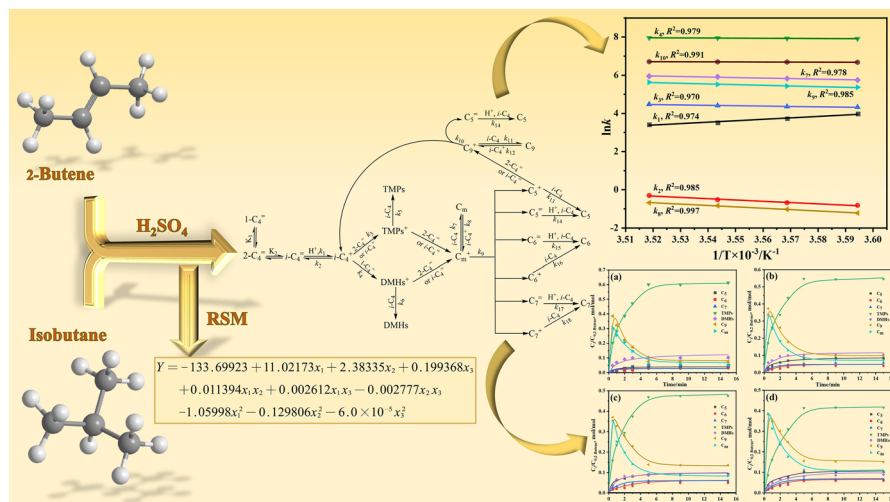
Introduction

With the issuance of new standards for gasoline use, the restrictions on the contents of aromatics, olefins and sulfur in gasoline have become more stringent, and there is an urgent need to develop clean, high-quality gasoline blending components that are required to have high octane values, yet control the introduction of aromatics, olefins, and sulfur to meet environmental requirements [1–4]. In petrochemical production, the alkylation reaction is an essential process, which uses isobutane and C_4 olefins as reaction materials and strong acids as catalysts to produce alkylates [5–7]. The alkylated oil has a high octane value, low sulfur content is free of alkenes and aromatics, and exhibits good explosive resistance, making it a highly desirable gasoline reconciling component [8–10]. Alkylated oils are one of the most vital gasoline blending components, which not only increase the octane number but also reduce the content of other components in gasoline. Identifying alkylated oils as gasoline blending components can greatly reduce the levels of sulfur, alkenes and aromatics in gasoline. With the rapid development of the automotive industry, gasoline with good antiknock performance and high octane number has been increasingly valued [11, 12].

Presently, the catalysts used for the alkylation reaction of isobutane are liquid acids, ionic liquids and solid acids. Among them, sulfuric acid and hydrofluoric acid are the liquid acid catalysts that are widely used in industrial production at present, with H_2SO_4 being adopted more than HF for safety issues. However,

H_2SO_4 and HF have significant safety, corrosiveness, recyclability and sustainability issues, which are the drawbacks of liquid acid catalysts that need continuous improvement [13–17]. The ionic liquid, as an efficient, environmentally friendly and sustainable catalyst, can surmount some of the problems in traditional liquid acid, which is considered an alternative to traditional alkylation catalysts to provide a sustainable route to clean oil for refineries. There are some plants have already commercialised the ionic liquid alkylation process, and the ionic liquid may replace H_2SO_4 as the mainstream alkylation process catalyst in the future [18]. Notwithstanding the good potential of the ionic liquid alkylation process, there are still some unresolved issues such as high viscosity, high cost, and complex preparation, which limit its widespread application in commercialization [19]. Up to now, the industrial production of alkylated oils in the world is still dominated by the sulfuric acid process, and continuing the in-depth study of the sulfuric acid alkylation reaction is still of great importance.

The investigation of isobutane alkylation reactions was based on a mechanism based on the ionic principle proposed by Schmerling in the 1940s to depict the process of alkylation involving olefins and isobutane [20, 21]. Since then, the carbonium ions theory has been rapidly developed. Subsequently, Albright et al. [22, 23] revealed that the main route for the production of dimethylhexane (DMHs) was not the isomerization of trimethylpentane ions. Kramer [24] demonstrated that the critical step affecting the rate of the alkylation reaction was due to the hydride transfer reaction. Sun et al. [25] constructed a model for the kinetics of the isobutane/butene alkylation reaction and used the model to predict the variation of major component concentrations with time. Li et al. [26] determined the concentrations of the major components of the isobutane/2-butene alkylation using a special microreactor and built a model for the kinetics involving the primary and secondary reactions. The isobutane/2-butene alkylation is a complicated reacion along with numerous side reactions. The current study focuses on the main reaction and does not deeply investigate how the side reactions in it are specifically allowed to occur. Therefore, continued research on the reaction kinetics of isobutane/2-butene reactions is important to refine the mechanism of alkylation reactions with guidance on the design of industrial reactors.

In this study, the alkylation of the C_4 fraction was carried out using a self-designed batch reactor in which sulfuric acid was chosen as the catalyst. With a view to analyzing the impact of individual influencing factors on the major product, a univariate analysis was conducted on the reaction to preliminarily explore the relationship between predictor variables and response variables, and a multivariate analysis was conducted using response surface methodology (RSM), which can further exhaust the influence of other confounding factors, thus determining the correlation between predictor variables and response variables, and finally selecting the best response conditions. In addition, based on the analysis of the reaction process, a complex reaction path was proposed, and a new kinetic model was constructed to study the reaction kinetics of isobutane/2-butene.

Experiment and method

Materials

Sulfuric acid (96–98%) was obtained from Chengdu Kelon Chemical Co., Ltd. The high-purity nitrogen (N_2, 99.999%), hydrogen (H_2, 99.999%), dry air and isobutane/2-butene mixture (I/O = 10:1, mol: mol) were obtained from Guangdong Huate Gas Co., Ltd.

Experiments design and RSM optimization

According to the literature [27], the thermal conductivity of H_2SO_4 is higher than the hydrocarbon, which can effectively dissipate the heat of the reaction and reduce the side reactions when the acid serves as a continuous phase. The acid to hydrocarbon ratio (A/H) commonly used in industry is 1–1.5:1 to ensure that the sulfuric acid is in the continuous phase. Zhang et al. [28] studied the reaction parameters affecting the alkylation reaction catalyzed by H_2SO_4 and found that the catalytic performance of A/H varied little between 1.0 and 1.2, which indicated that an A/H of 1.0 was appropriate. Thus, in this study, we used 1:1 of A/H to study the isobutane/2-butene alkylation reaction.

In this work, the effects of temperature (3.0–11.0 °C), time (1.0–9.0 min) and stirring speed (900–1500 rpm) of the alkylation reaction on selectivity of TMPs were investigated respectively, with other conditions held constant. However, the traditional single-factor study is cumbersome and time-consuming. What's more, it ignores the interactions between various factors [29]. RSM is a method of applying mathematical models to statistical experiments that reduces measurements, increases the likelihood of statistical interpretation, and indicates the interactions between variables [30]. In this study, RSM was used together with a central composite design (CCD) to optimize several experimental conditions in a single-factor experiment.Then the interactions of each response factor and the extent of their respective effects were investigated. Therefore, the RSM can be applied to simulate the production process for the alkylation of isobutane/2-butene. The experiments were designed using three independent variables, such as reaction temperature (x_1), reaction time (x_2) and stirring speed (x_3). The quadratic polynomial model of the alkylate selectivity can be expressed by Eq. (1).

$$Y = \beta_0 + \sum_{i=1}^{k} \beta_i x_i + \sum_{i=1}^{k} \beta_{ii} x_i^2 + \sum_{i=1, i<j}^{k-1} \sum_{j=1}^{k} \beta_{ij} x_i x_j \tag{1}$$

where Y is the predicted value, x_i and x_j are the variables of the different factors, β_0 is the model constant, β_i, β_{ii}, and β_{ij} are the regression coefficients, k is the number of factor variables.

Analysis of variance (ANOVA) is mainly applied to test the sufficiency of various factors in the reaction. The value of F is used to examine the applicability of

modeling the experiment. Suppose the value of F calculated from the actual data is larger than that in the table of standard distributions. In that case, it means that the model has a good fit for accurately predicting the experimental results under different reaction conditions. Furthermore, the value of P 0.05 implies a significant effect within the 95.0% confidence interval, with a lower value of P indicating a more significant impact.

C$_4$ alkylation reaction

The alkylation experiments were carried out within a 0.1 L batch reactor. It was beneficial for the alkylation reaction to occur at low temperatures, so the refrigerant was circulated to obtain a refrigeration system, which allowed for the control of the reactor temperature. In order to keep the hydrocarbons in a liquid state while the reaction took place, the reactor pressure was set to 0.5 MPa. In the batch alkylation experiment, the catalyst of H_2SO_4 was added to the reactor, and then the reactor was sealed. Afterward, the reactor was vacuumed, and N_2 was flushed in to replace the air and repeated three times. Next, a quantity of N_2 was charged and held for 10 min to check for significant pressure changes in the reaction system to ensure the reactor was not leaking. As a set temperature level was reached in the reactor, the hydrocarbon feedstock was rapidly added to it. In the meantime, the stirrer was started to disperse the catalyst and the reaction material fully. Sampling was performed at the specified time according to the experimental requirements, and the samples were analyzed using the GC. The diagram of the experimental device is shown in Fig. 1.
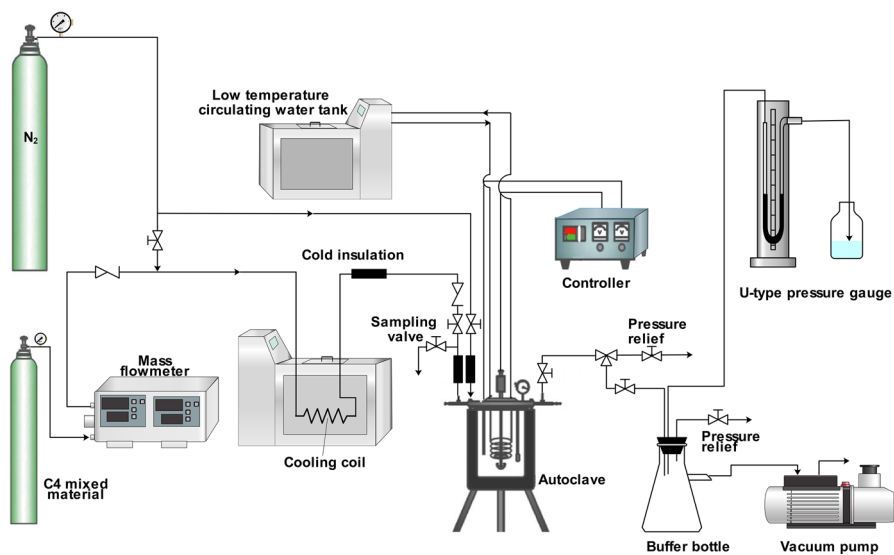

Fig. 1 Diagram of the experimental setup for C_4 alkylation reaction

Results and discussion

Single-factor study results

The alkylation gas phase products at different reaction times were analyzed to define the 2-butene mass fraction, the 2-butene conversion at different times can be calculated according to Eq. (2). The results are shown in Fig. S1.

$$x_{2-butene} = \frac{x_{in,2-butene} - x_{out,2-butene}}{x_{in,2-butene}} \times 100\% \qquad (2)$$

where $x_{2\text{-butene}}$ represents the 2-butene conversion, $x_{in,2\text{-butene}}$ indicates the 2-butene mass fraction before the reaction, and $x_{out,2\text{-butene}}$ denotes the 2-butene mass fraction after the reaction.

As seen in Fig. S1, the 2-butene conversion was already 97.12% in 2 min, indicating that the 2-butene was mostly consumed within 2 min. There was a slight increase in the 2-butene conversion following 2 min of the reaction, reaching 98.08% during 5 min. The conversion rate no longer changed after 5 min but was not 100%, which may be due to the presence of saturated vapor pressure under the reaction conditions of 2-butene, failing to participate in the reaction fully. In the following study, the conversion of 2-butene will not be elaborated on separately. If not specifically labeled, the conversion of 2-butene is considered to be 98.08%.

Selective influence of time on TMPs

As shown in Fig. S2, in the conditions of reaction time of 1–15 min, reaction temperature set at 7 °C, stirring speed of 1300 rpm, reaction pressure of 0.5 MPa and A/H of 1:1, the selectivity of TMPs first increased sharply with increasing reaction time and then gradually remained stable. As the reaction temperature increased from 3 to13 °C, with the corresponding change in the selectivity of TMPs from 14.25 to 54.51%. During 0.5 and 2 min, there was a dramatic increase in TMPs selectivity; the rate of increase gradually slowed down within 2 to 5 min; after 5 min, the TMPs selectivity had leveled off. This indicates that the C_4 alkylation reaction mainly occurred in the first 2 min. The isomerization of other components from 2 to 5 min mainly produced TMPs, while the reaction ended after 5 min. Therefore, the median reaction time of the RSM test design in this paper was 5 min, the maximum reaction time was set to 9 min, and the minimum reaction time was set to 1 min.

Selective influence of temperature on TMPs

The reaction time was kept at 5 min, the stirring speed was 1300 rpm, the reaction pressure was 0.5 MPa, and the A/H was 1:1. The different reaction temperatures of 3–13 °C were chosen to investigate the effect on the selectivity of TMPs. The results of the experiments are displayed in Fig. S3. The selectivity of TMPs decreases with increasing temperature within the specified reaction temperature. As the temperature

rose from 3 to 13 °C, the TMPs selectivity consequently changed from 66.50 to 36.05%. Since high temperatures favor side reactions such as oligomerization/cleavage reactions, increased by-products reduce the selectivity of the main product TMPs. In addition, it was reported in the literature that if the reaction temperature is too low, the viscosity of the concentrated sulfuric acid catalyst increases, which is not favorable for the reaction [31]. Low temperature can improve the selectivity of TMPs, but the reaction temperature should not be too low. The reaction temperature of most conventional mechanically stirred alkylation reactors is around 7 °C. Therefore, in this paper, a reaction temperature of 7 °C was taken as the median value for the RSM experimental design, with the highest temperature of 11 °C and the lowest temperature of 3 °C.

Selective influence of stirring speed on TMPs

The effect of stirring speed on the selectivity of TMPs was investigated at a reaction time of 5 min, a reaction temperature of 7 °C, a reaction pressure of 0.5 MPa, an A/H of 1:1, and a stirring speed of 700–1700 rpm. The outcomes of the experiment are displayed in Fig. S4. The TMPs selectivity rose as stirring speed increased, but the selectivity of TMPs increased slowly after the stirring speed reached 1300 rpm. With a rise in stirring speed from 700 to 1700 rpm, the selectivity of TMPs changed correspondingly from 17.00 to 61.11%. It is mainly caused by the effect of dispersion between the hydrocarbon feedstock and H_2SO_4. Increasing the speed can increase the degree of dispersion between the acid hydrocarbons, which is conducive to the occurrence of the primary alkylation reaction and reduce the generation of by-products. Considering the capacity of this equipment and energy consumption, 1300 rpm was taken as the median value of the stirring speed factor in the RSM test design. The maximum and minimum values were 1700 rpm and 900 rpm, respectively.

Optimization of RSM

RSM modeling

The RSM, first proposed by British mathematicians G. Box and Wilson in 1951, is a statistical method involving the design of experiments and statistics for the design, development, improvement and optimization of processes [32, 33]. It is often used to study how the target response value is affected by multiple factors and assess the extent to which different factors affect the response value and the interactive effects among the elements.

The correlation between the variables in the experimental procedure and the selectivity of the TMPs was investigated by the Central Composite Design (CCD) RSM modeling with 20 runs. The running results for the RSM model are displayed in Table 1.The experimental values are the average values obtained after three repetitions. The maximum residual of the 20 validation experiments was 1.56%.

Table 1 Experimental and predicted results of TMPs production with C_4 alkylation reaction

Run order	Reaction time (min)	Reaction temperature (℃)	Stirring speed (rpm)	Experimental selectivity of TMPs (%)	Predictive selectivity of TMPs (%)
1	7	5	1100	51.07	52.09
2	5	7	1300	54.51	55.07
3	3	9	1500	39.10	39.32
4	3	9	1100	29.05	28.86
5	5	7	1300	55.71	55.07
6	5	7	1700	61.11	60.23
7	3	5	1500	52.56	53.58
8	5	7	1300	55.31	55.07
9	5	7	900	31.05	30.70
10	5	7	1300	54.28	55.07
11	7	9	1100	42.24	42.45
12	5	7	1300	55.76	55.07
13	3	5	1100	37.79	38.68
14	7	5	1500	69.74	71.17
15	9	7	1300	54.58	53.69
16	5	3	1300	66.50	64.94
17	5	11	1300	40.71	41.04
18	7	9	1500	56.74	57.09
19	5	7	1300	56.06	55.07
20	1	7	1300	22.87	22.52

The fitting effect is assessed with the regression coefficient (R^2) for the RSM model. The R^2 of the model obtained in this work is 0.9958, which indicates that the mathematical model fits well and accurately represent the overall relation between the response values and all elements. As shown in Fig. S5, there was a high correlation between the model predictions and the experimental values, indicating that the established model provided accurate results. Equation (3) could be used to express the relationship between TMPs selectivity and elements according to Table 1 and Eq. (1).

$$
\begin{aligned}
Y = {} & -133.69923 + 11.02173x_1 + 2.38335x_2 + 0.199368x_3 \\
& + 0.011394x_1x_2 + 0.002612x_1x_3 - 0.002777x_2x_3 \\
& - 1.05998x_1^2 - 0.129806x_2^2 - 6.0 \times 10^{-5}x_3^2
\end{aligned} \tag{3}
$$

where Y is the target response value, i.e., the selectivity of the TMPs; x_1, x_2, x_3 are the experimental data of reaction time, reaction temperature and stirring speed, respectively.

Analysis of variance (ANOVA)

The ANOVA indicated that single parameters and parameter interactions had a great influence here on reaction. The suitability of the model was tested using the values of F. As shown in Table 2, the value of F for the developed model was 264.77, and a value of P less than 0.0001, indicating that it was significant as the risk of the "F-value of the model" becoming larger caused by noise was 0.01%. The values of P were used to determine the significance of the effects caused by different elements upon a response value. If the P-value was ≤ 0.05, it indicated that the factor significantly affected the response value; otherwise, the item was not statistically significant. The results revealed that all terms in the model had significant effects on the selectivity of TMPs except for $x_1 x_2$, with x_1 being the most significant model term.

In addition, the predicted R_{pre}^2 value in the conducted experiments was 0.9721, which indicated the anticipated and practical results were rather well in accord. The signal-to-noise ratio was represented by the model's Adeq Precision (AP), and it showed that the model was workable with $AP = 61.77 > 4$. The lack of fit is essential data used to assess the reliability of the equation; if it is significant means that the equation is poorly simulated and needs to be adjusted; if it is insignificant indicates that the equation is relatively well simulated and can be well analyzed for future data. In this work, The lack of fit term was not statistically significant ($P = 0.0863 > 0.05$), indicating that the data could be well described by the model. The coefficient of variation (C.V. $= 2.62\% < 15\%$) of the model was comparatively small, indicating the experiment had excellent precision and reliability.

Table 2 ANOVA for the RSM quadratic model of selectivity of TMPs

Source	Sum of squares	Degrees of freedom	Mean square	F-value	P-value
Model	2956.15	9	328.46	264.77	<0.0001
x_1	972.01	1	972.01	783.52	<0.0001
x_2	571.2	1	571.2	460.43	<0.0001
x_3	872.03	1	872.03	702.93	<0.0001
$x_1 x_2$	0.0166	1	0.0166	0.0134	0.9102
$x_1 x_3$	8.73	1	8.73	7.04	0.0242
$x_2 x_3$	9.87	1	9.87	7.96	0.0181
x_1^2	451.99	1	451.99	364.34	<0.0001
x_2^2	6.78	1	6.78	5.46	0.0415
x_3^2	144.96	1	144.96	116.85	<0.0001
Residual	12.41	10	1.24		
Lack of Fit	9.8	5	1.96	3.76	0.0863
Pure Error	2.61	5	0.5215		
Cor Total	2968.55	19			
Std. Dev	1.11		R^2	0.9958	
C.V. %	2.26		R_{pre}^2	0.9721	
Adeq Precision	61.77		R_{adj}^2	0.9921	

Optimization of C$_4$ alkylation reaction conditions

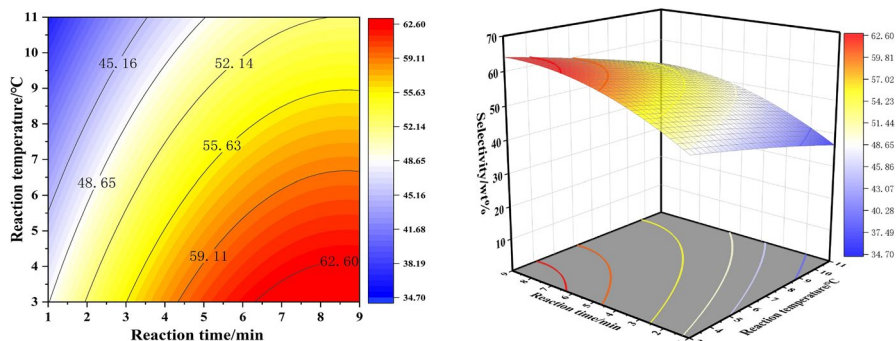### Response surface plots of C$_4$ alkylation reaction

The fitted regression model was used to plot the three-dimensional (3D) response surface curves. They better visualized the effects of various factors interacted with one another and the response results. The degree of significance of the response values for various parameters was expressed in the sparsity or density of the 3D response surface curves. In this study, 3D surface curves were used to visually depict how the reaction temperature, reaction time, and stirring rate affected the selectivity of TMPs.

The interaction between the reaction temperature and reaction time at a stirring speed of 1300 rpm is shown Fig. 2. The selectivity of TMPs was low at slightly higher reaction temperatures and increased as the temperature decreased; the selectivity of TMPs increased with increasing reaction time and finally stabilized. It was observed that the interaction between reaction temperature and reaction time was less significant ($P = 0.9102 > 0.05$).

The interaction between reaction time and stirring speed at 7 °C is depicted in Fig. 3. As seen in the figure, the selectivity of TMPs was increased with the increase in stirring speed. This may be due to the fact that the high rate of stirring disperses the acid hydrocarbon sufficiently, which will enhance the reaction and produce more target products. In contrast, the longer reaction time will allow the system to react sufficiently and finally reach equilibrium. The interaction was observed to be pretty significant ($P = 0.0242 < 0.05$).

Fig. 4 illustrates the association between reaction temperature and stirring speed and the selectivity of TMPs at 5 min of the reaction. The figure showed that the selectivity of TMPs rose as reaction temperature decreased. A decrease in the octane number of the alkylated oil was observed as a result of the study's findings that raising the reaction temperature during the alkylation reaction caused an increase in the content of by-products like isomerization in the alkylation

Fig. 2 Contour plot and response surface plot of TMPs vs. reaction time and reaction temperature (N = 1300 rpm, A/H = 1:1)
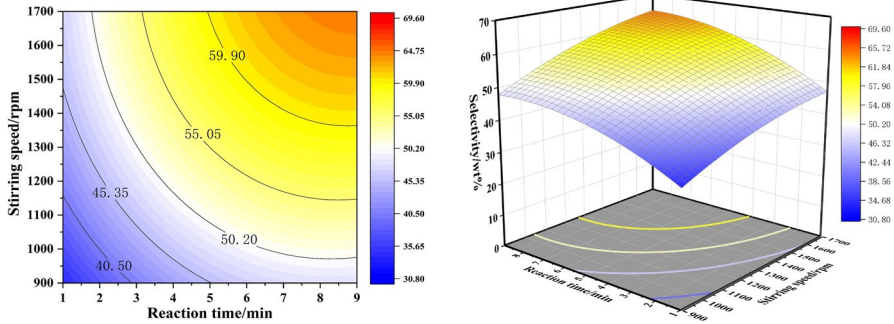
Fig. 3 Contour plots and response surface plots of TMPs vs. reaction time and stirring speed (T = 7 °C, A/H = 1:1)
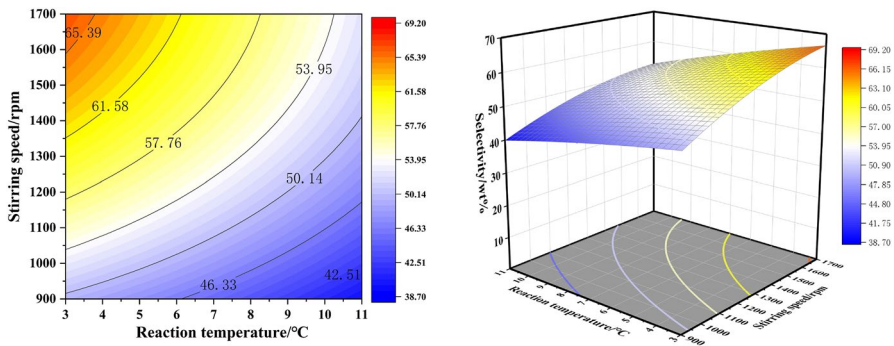
Fig. 4 Contour plots and response surface plots of TMPs vs. reaction temperature and stirring speed (t = 5 min, A/H = 1:1)

products; decreasing the reaction temperature increases the content of TMPs. It was observed that this interaction had a significant effect. ($P = 0.0181 < 0.05$).

Optimization reaction conditions

For this work, at reaction conditions of 3 °C, 7 min, and 1500 rpm, the best selectivity of TMPs predicted by the model was 76.72%. The experiment was conducted three times under the response surface model's optimum conditions to check the model's accuracy, and the average selectivity was 77.47%. The relative error between the anticipated and experimental averages was 0.98%. Therefore, the proposed model is reasonable. Table 3 presents the experimental outcomes.

Table 3 Prediction optimization validation results

| Response value	Number			Average value	Predicted value	Relative error
	1	2	3			
Selectivity/wt%	77.65	76.64	78.13	77.47	76.72	0.98%

Kinetic model

Model building

The alkylation process is a very quick reaction. Sulfuric acid at low temperatures can have a significant impact on the mass transfer when the transfer rate is insufficient [34]. The mass transfer limitation had been abolished because it had been demonstrated experimentally that, after the stirring speed exceeded 1300 rpm, raising the stirring speed had minimal impact on the alkylation process. Thus, 1300 rpm stirring speed was used throughout all investigations on alkylation kinetics at varying temperatures.

A thorough understanding of the reaction mechanism is essential since it is crucial to the design and optimization of the reaction process. The mechanism of the alkylation reaction has received a lot of attention. The classical carbenium ion mechanism is a commonly accepted explanation for the sulfuric acid alkylation process.

The classical carbenium ion mechanism applies to the alkylation of isobutane and olefins. At first, Isobutylene undergoes a reversible protonation reaction with a strong acid in an acidic environment to produce the tert-butyl group.

$$i - C_4^= + H^+ \underset{k_2}{\overset{k_1}{\rightleftharpoons}} i - C_4^+ \tag{4}$$
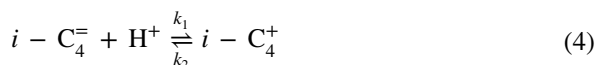
where $i\text{-}C_4^=$ is isobutylene and $i\text{-}C_4^+$ is the tert-butyl group.

In the existence of H_2SO_4, isomerization reactions between various olefins occur rapidly, and the thermodynamic equilibrium between several olefins is more inclined to produce isobutene. The equation of the isomerization reaction is shown below.

$$1 - C_4^= \overset{K_1}{\rightleftharpoons} 2 - C_4^= \overset{K_2}{\rightleftharpoons} i - C_4^= \tag{5}$$
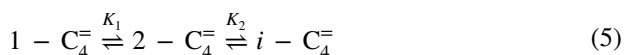
where $1\text{-}C_4^=$ is 1-butene; $2\text{-}C_4^=$ is 2-butene; K_1 is the reaction equilibrium constant of 2-butene with 1-butene; K_2 is the reaction equilibrium constant of 2-butene with isobutene.

The tert-butyl group reacts with isobutene (or 2-butene) to create the C_8 carbonium ion, which further interacts with isobutane to create 2,2,4-trimethylpentane and the tert-butyl group by a hydrogen transfer process.

The tert-butyl group reacts with isobutene (or 2-butene) to produce the C_8 carbonium ion, which continues to interact with isobutane by hydrogen transfer reaction to obtain 2,2,4-trimethylpentane and the tert-butyl group. The tert-butyl group is rejoined in the catalytic reaction cycle.

$$i - C_4^+ + i - C_4^= (or\ 2 - C_4^=) \xrightarrow{k_3} TMPs^+ \tag{6}$$

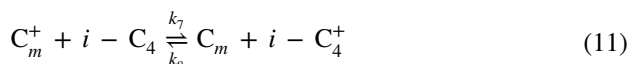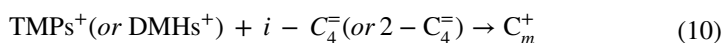$$TMPs^+ + i - C_4 \xrightarrow{k_5} TMPs + i - C_4^+ \tag{7}$$
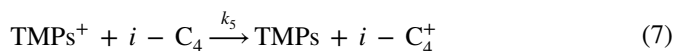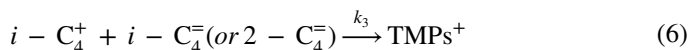
where TMPs is represented by trimethylpentane. The C_8 carbenium ion can undergo isomerization reactions through methyl and hydride transfers to afford various C_8 carbenium ions.

The formation pathway of the DMHs is similar to that of the TMPs. The tert-butyl group reacts with 1-butene to create the DMHs, where DMHs is indicated as dimethylpentane.

$$i - C_4^+ + 1 - C_4^= \xrightarrow{k_4} DMHs^+ \tag{8}$$

$$DMHs^+ + i - C_4 \xrightarrow{k_6} DMHs + i - C_4^+ \tag{9}$$
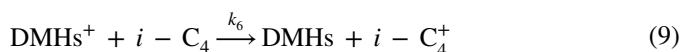
The polymer cations (C_m^+, $m \geq 10$) are mainly produced by the polymerization of olefins or synthesized by $TMPs^+$ (or $DMHs^+$) with $i-C_4^=$ (or $2-C_4^=$). Then C_m^+ continues to react with $i-C_4$ to produce C_m and $i-C_4^+$.

$$TMPs^+ (or\ DMHs^+) + i - C_4^= (or\ 2 - C_4^=) \rightarrow C_m^+ \tag{10}$$

$$C_m^+ + i - C_4 \underset{k_8}{\overset{k_7}{\rightleftharpoons}} C_m + i - C_4^+ \tag{11}$$
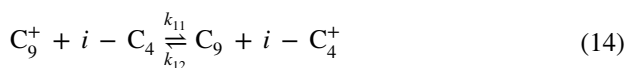
The long-chain carbocations are unstable in an acidic environment, and they undergo cleavage reactions to form more stable molecules. Thus C_m^+ will fragment into different small molecules of olefins or carbocations.

$$C_m^+ \xrightarrow{k_9} C_x^+ + C_y^= \tag{12}$$

where C_x^+ represents the carbenium ion and $C_y^=$ means olefin, $x, y = 5, 6, 7$.

Since C_9^+ is less stable, a fraction breaks to generate $C_5^=$ and $i-C_4^+$; The other moiety would react with i-C_4 to produce C_9, which is a reversible reaction.

$$C_9^+ \xrightarrow{k_{10}} C_5^= + i - C_4^+ \tag{13}$$

$$C_9^+ + i - C_4 \underset{k_{12}}{\overset{k_{11}}{\rightleftharpoons}} C_9 + i - C_4^+ \tag{14}$$
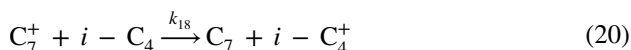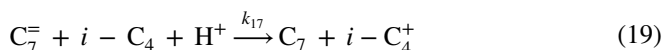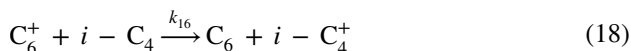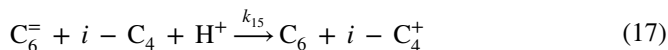
The $C_5^=$ and C_5^+ generated by the breakage of the long-chain carbenium ions will further react in an acidic environment to form C_5.

$$C_5^= + i - C_4 + H^+ \xrightarrow{k_{13}} C_5 + i - C_4^+ \tag{15}$$

$$C_5^+ + i - C_4 \xrightarrow{k_{14}} C_5 + i - C_4^+ \tag{16}$$
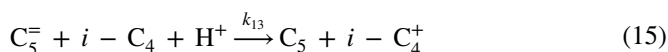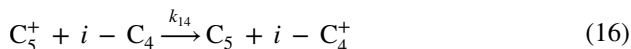
The $C_6^=$ and C_6^+, $C_7^=$ and C_7^+ generated by the fracture of long-chain carbenium ions will also undergo similar reactions, producing C_6 and C_7, respectively.

$$C_6^= + i - C_4 + H^+ \xrightarrow{k_{15}} C_6 + i - C_4^+ \tag{17}$$

$$C_6^+ + i - C_4 \xrightarrow{k_{16}} C_6 + i - C_4^+ \tag{18}$$

$$C_7^= + i - C_4 + H^+ \xrightarrow{k_{17}} C_7 + i - C_4^+ \tag{19}$$

$$C_7^+ + i - C_4 \xrightarrow{k_{18}} C_7 + i - C_4^+ \tag{20}$$

In summary, Fig. 5 depicts the entire reaction route network.

During the process of alkylation, numerous side reactions occur simultaneously, so that many isoalkanes and the corresponding carbenium ions. Moreover, the intramolecular hydrogen transfer and intramolecular methyl transfer lead to the generation of a large number of isomers. However, only a few key groups can be measured in alkylations, and carbon ions are challenging to detect. To avoid overfitting, we try to simplify the model. The TMPs, DMHs and C_m are each defined as a single component. In addition, it is assumed that the alkylation reaction is in chemical equilibrium before the
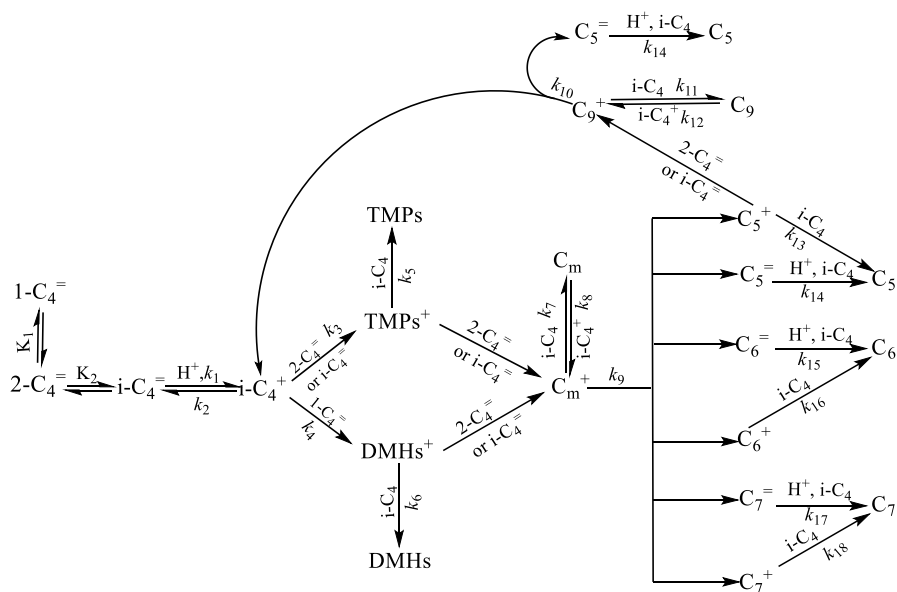
Fig. 5 Diagrammatic representation of the reaction pathway network

occurrence of Eq. (5). Thus, using the total concentration of olefins, it is possible to calculate the concentration distributions of isobutene, 1-butene, and 2-butene individually.

$$c_{1-C_4^=} = \alpha \cdot c_{2-C_4^=} \tag{21}$$

$$c_{i-C_4^=} = \beta \cdot c_{2-C_4^=} \tag{22}$$

where $\alpha = K_1/(1+K_1+K_2)$, $\beta = K_2/(1+K_1+K_2)$.

The following kinetic model will be constructed using the reaction stages and postulates previously given,

$$\begin{aligned}
\frac{dc_1}{dt} =\ & k_2 c_3 - k_1 \beta c_1 - k_3(1-\alpha)c_1 c_3 - k_4 \alpha c_1 c_3 - k_7(1-\alpha)c_1 c_2 c_4 \\
& - k_7(1-\alpha)c_1 c_2 c_5 - k_{10}(1-\alpha)c_1 c_{11} - k_{11}(1-\alpha)c_1 c_2 c_{11}
\end{aligned} \tag{23}$$

$$\begin{aligned}
\frac{dc_2}{dt} =\ & k_8 c_3 c_8 + k_{12} c_3 c_{18} - k_5 c_2 c_4 - k_6 c_2 c_5 - k_7(1-\alpha)c_1 c_2 c_4 \\
& - k_7(1-\alpha)c_1 c_2 c_5 - k_{11}(1-\alpha)c_1 c_2 c_{11} - k_{13} c_2 c_{11} \\
& - k_{14} c_2 c_{10} - k_{15} c_2 c_{13} - k_{16} c_2 c_{14} - k_{17} c_2 c_{16} - k_{18} c_2 c_{17}
\end{aligned} \tag{24}$$

$$\begin{aligned}
\frac{dc_3}{dt} =\ & k_1 \beta c_1 - k_2 c_3 - k_3(1-\alpha)c_1 c_3 - k_4 \alpha c_1 c_4 - k_8 c_3 c_8 - k_{12} c_3 c_{18} \\
& + k_{10}(1-\alpha)c_1 c_{11} + k_5 c_2 c_4 + k_6 c_2 c_5 + k_7(1-\alpha)c_1 c_2 c_4 \\
& + k_7(1-\alpha)c_1 c_2 c_5 + k_{11}(1-\alpha)c_1 c_2 c_{11} + k_{13} c_2 c_{11} + k_{14} c_2 c_{10} \\
& + k_{15} c_2 c_{13} + k_{16} c_2 c_{14} + k_{17} c_2 c_{16} + k_{18} c_2 c_{17}
\end{aligned} \tag{25}$$

$$\frac{dc_4}{dt} = k_3(1-\alpha)c_1 c_3 - k_5 c_2 c_4 - k_7(1-\alpha)c_1 c_2 c_4 - k_9(1-\alpha)c_1 c_4 \tag{26}$$

$$\frac{dc_5}{dt} = k_4(1-\alpha)c_1 c_3 - k_6 c_2 c_5 - k_7(1-\alpha)c_1 c_2 c_5 - k_9(1-\alpha)c_1 c_5 \tag{27}$$

$$\frac{dc_6}{dt} = k_5 c_2 c_4 \tag{28}$$

$$\frac{dc_7}{dt} = k_6 c_2 c_5 \tag{29}$$

$$\frac{dc_8}{dt} = k_7(1-\alpha)c_1 c_2 c_4 + k_7(1-\alpha)c_1 c_2 c_5 - k_8 c_3 c_8 \tag{30}$$

$$\frac{dc_9}{dt} = k_{13}c_2c_{11} + k_{14}c_2c_{10} \tag{31}$$

$$\frac{dc_{10}}{dt} = k_9(1 - \alpha)c_1c_4 + k_9(1 - \alpha)c_1c_5 + k_{10}(1 - \alpha)c_1c_{11} - k_{14}c_2c_{10} \tag{32}$$

$$\frac{dc_{11}}{dt} = k_9(1 - \alpha)c_1c_4 + k_9(1 - \alpha)c_1c_5 + k_{10}(1 - \alpha)c_1c_{11} - k_{13}c_2c_{11} \tag{33}$$

$$\frac{dc_{12}}{dt} = k_{15}c_2c_{13} + k_{16}c_2c_{14} \tag{34}$$

$$\frac{dc_{13}}{dt} = k_9(1 - \alpha)c_1c_4 + k_9(1 - \alpha)c_1c_5 + k_{10}(1 - \alpha)c_1c_{11} - k_{15}c_2c_{13} \tag{35}$$

$$\frac{dc_{14}}{dt} = k_9(1 - \alpha)c_1c_4 + k_9(1 - \alpha)c_1c_5 + k_{10}(1 - \alpha)c_1c_{11} - k_{16}c_2c_{14} \tag{36}$$

$$\frac{dc_{15}}{dt} = k_{17}c_2c_{16} + k_{18}c_2c_{17} \tag{37}$$

$$\frac{dc_{16}}{dt} = k_9(1 - \alpha)c_1c_4 + k_9(1 - \alpha)c_1c_5 + k_{10}(1 - \alpha)c_1c_{11} - k_{17}c_2c_{16} \tag{38}$$

$$\frac{dc_{17}}{dt} = k_9(1 - \alpha)c_1c_4 + k_9(1 - \alpha)c_1c_5 + k_{10}(1 - \alpha)c_1c_{11} - k_{18}c_2c_{17} \tag{39}$$

$$\frac{dc_{18}}{dt} = k_{11}(1 - \alpha)c_1c_2c_{11} - k_{12}c_3c_{18} \tag{40}$$

where the initial conditions are zero components except for $t=0$, $c_1=c_1^0$; $c_2=c_2^0$. In Eqs. (23)–(40), the number 1 to 18 is related to the corresponding species as follows: 1, 2-C$_4^=$; 2, i-C$_4$; 3, i-C$_4^+$; 4, TMPs$^+$; 5, DMHs$^+$; 6, TMPs; 7, DMHs; 8, C$_m$; 9, C$_5$; 10, C$_5^=$; 11, C$_5^+$; 12, C$_6$; 13, C$_6^=$; 14, C$_6^+$; 15, C$_7$; 16, C$_7^=$; 17, C$_7^+$; 18, C$_9$.

Estimation methods and results

Before fitting the system of ordinary differential equations, the constants α and β in the system of equations need to be determined. Therefore, it is necessary to calculate the equilibrium constants (K_1 and K_2) for the isomerization reaction of 2-butene. The parameters of K_1 and K_2 at various temperatures can be calculated using the RGibbs block on the ASPEN Plus platform's robust thermodynamic

Table 4 Concentration distribution and equilibrium constants of butane

Temperature/K	1-C$_4^=$/%	cis-2-C$_4^=$/%	trans-2-C$_4^=$/%	i-C$_4^=$/%	K$_1$	K$_2$
278.2	0.37	3.47	9.23	86.93	0.0291	6.8425
280.2	0.39	3.57	9.38	86.66	0.0300	6.6935
282.2	0.41	3.66	9.53	86.40	0.0309	6.5497
284.2	0.43	3.76	9.67	86.14	0.0317	6.4110

database. The average of the equilibrium constants obtained from the RGibbs block could be applied to determine the values of α and β. The calculation results of the equilibrium constants are displayed in Table 4.

The average K$_1$ and K$_2$ between 278.2 and 284.2 K can be obtained from Table 4 as 0.0304 and 6.6242, respectively. Thus, according to Eqs. (21) and (22), one can obtain α and β as 0.0040 and 0.8654, respectively.

The estimation of parameters is actually the optimization of the data, and the determination of the optimization objective is a significant step. Optimization techniques used for parameter estimation usually require a valid error statistical criterion. A suitable error criterion, such as least squares, maximum likelihood, and probability density functions, can be used to predict the system's ideal parameters. For most nonlinear parameter estimation problems, the optimization criterion uses the least squares method to obtain a satisfactory optimal solution.

In this paper, the kinetic model for the alkylation process of isobutane/2-butene was developed where catalyst was sulfuric acid, and the program code was written in Matlab programming language for the calculation. The ODE45 function in Matlab was applied to resolve the system of ordinary differential Eqs. (23)–(40). The Runge–Kutta method was used for iterative calculations to fit the estimated parameters by nonlinear least squares, i.e., the following objective function was fitted by nonlinear least squares, as shown in Eq. (41).

$$F = \sum_{i=1}^{n} \left(c_{i,cxp} - c_{i,cal} \right)^2 \tag{41}$$

where n is the quantity of experimental data, and $c_{i,exp}$ and $c_{i,cal}$ stand for the experimental and calculated data of component i, respectively.

During the fitting calculations, it was found that k_5, k_6 and k_{11}-k_{18} had little variation with temperature, indicating that these reaction steps had extremely low activation energies. Langley et al. [23] also found this phenomenon during their study, stating that the reason for this is that these rate constants are not a function of temperature. This phenomenon also indicates that the hydride transfer reaction is not a strong function of temperature. Therefore, the values of these ten reaction rate constants are assumed not to vary with temperature to decrease the fraction of parameters to be adjusted, to simplify the fitting process, and to avoid the problem of overfitting.

Table 5 Kinetic rate constants and confidence intervals

| Rate constants	Temperature/K			
	278.2	280.2	282.2	284.2
k_1/ min^{-1}	52.67 ± 23.51	41.31 ± 11.17	33.29 ± 7.92	30.02 ± 4.81
k_2/min^{-1}	0.43 ± 0.04	0.50 ± 0.02	0.58 ± 0.01	0.73 ± 0.01
k_3/mol·mol^{-1}·min^{-1}	74.73 ± 28.42	76.90 ± 24.23	80.98 ± 9.47	86.45 ± 5.37
k_4, 10^3/mol·mol^{-1}·min^{-1}	2.71 ± 1.54	2.76 ± 0.67	2.81 ± 0.27	2.84 ± 0.18
k_5/mol·mol^{-1}·min^{-1}	32.41 ± 22.61			
k_6, 10^2/mol·mol^{-1}·min^{-1}	5.07 ± 0.95			
k_7, 10^2/mol^2·mol^{-2}·min^{-1}	3.10 ± 1.45	3.36 ± 2.29	3.66 ± 1.16	3.79 ± 0.61
k_8/mol·mol^{-1}·min^{-1}	0.29 ± 0.03	0.35 ± 0.01	0.43 ± 0.01	0.50 ± 0.01
k_9, 10^2/mol·mol^{-1}·min^{-1}	2.11 ± 1.48	2.26 ± 0.81	2.46 ± 0.69	2.75 ± 0.47
k_{10}, 10^2/mol·mol^{-1}·min^{-1}	7.86 ± 0.91	7.96 ± 0.62	8.04 ± 0.35	8.11 ± 0.15
k_{11}, 10^3/mol^2·mol^{-2}·min^{-1}	2.65 ± 1.10			
k_{12}/mol·mol^{-1}·min^{-1}	0.42 ± 0.01			
k_{13}/mol·mol^{-1}·min^{-1}	22.48 ± 0.27			
k_{14}, 10^2/ kg·mol^{-1}·min^{-1}	1.68 ± 1.07			
k_{15}/mol·mol^{-1}·min^{-1}	28.36 ± 0.01			
k_{16}/mol·mol^{-1}·min^{-1}	53.27 ± 0.01			
k_{17}/mol·mol^{-1}·min^{-1}	35.82 ± 0.14			
k_{18}/mol·mol^{-1}·min^{-1}	35.48 ± 0.13			

The estimated parameters and 95% confidence intervals for k_1-k_{18} were shown in Table 5. As Table 5 indicated, the confidence intervals for the majority of the parameters were one order of magnitude less than the respective parameters, which demonstrated the estimated rate constants were reliable. The concentration profiles predicted by the model, along with the measured value of the vital components for the alkylation reactants at various temperatures, were displayed in Fig. 6. The strong agreement between experimental results and expected values was immediately obvious, further demonstrating the dependability of kinetic model.

The Arrhenius relationship can be employed to determine the reaction's activation energy and pre-exponential factor, which is calculated as shown in Eqs. (42) and (43). The linear relationship between ln$k$ and 1/T for different rate constants was plotted based on Eq. (43). Fig. 7 displays the excellent linear correlation between ln$k$ and 1/T. However, the anti-Arrhenius behavior of k_1 can be observed in the figure, where the value of k_1 decreases with increasing temperature. This phenomenon may not be anomalous for hydrocarbon reactions in molecules with free radicals [35]. A decline in the multi-step reaction's equilibrium constant or variations in the environment may cause the anti-Arrhenius behavior [36, 37].

$$k = Ae^{\left(-\frac{E_a}{RT}\right)} \tag{42}$$
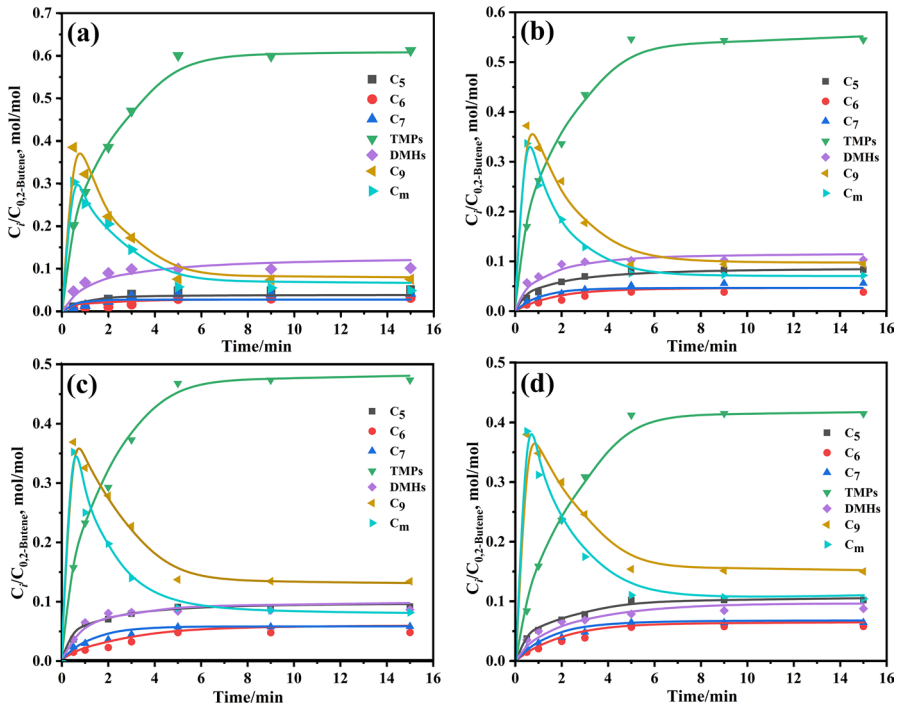
Fig. 6 Concentration distribution of critical components for the alkylation reaction of isobutene/2-butene. Temperature: **a** 278.2 K, **b** 280.2 K, **c** 282.2 K, **d** 284.2 K (N = 1300 rpm, A/H = 1:1). The symbols represent the experimental data and the lines indicate the fitted values of the kinetic model
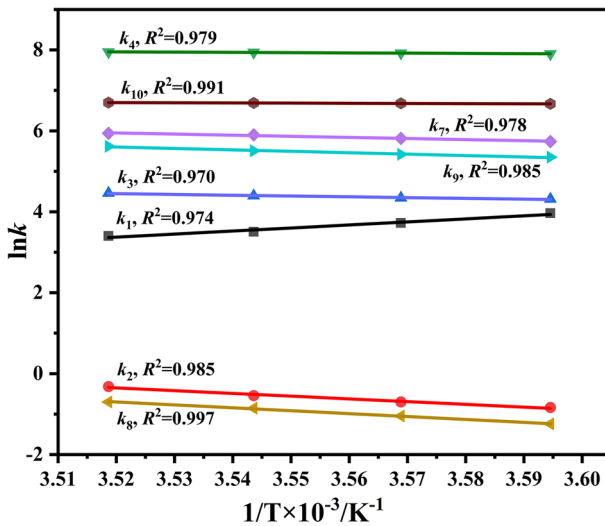
Fig. 7 The Arrhenius relationship of $\ln(k_i)$ and T^{-1}

Table 6 Activation energies (E_a) and pre-exponential factors (A) of the reaction

Rate constants	Activation energies, kJ/mol	Pre-exponential factors
k_1	− 62.59	9.07×10^{-11}
k_2	56.15	1.48×10^{10}
k_3	16.05	7.64×10^{4}
k_4	5.27	2.65×10^{4}
k_7	22.63	5.54×10^{6}
k_8	59.94	5.23×10^{10}
k_9	29.12	6.11×10^{7}
k_{10}	3.42	3.46×10^{3}

$$\ln k = -\frac{E_a}{R} \cdot \frac{1}{T} + \ln A \tag{43}$$

As can be seen from Table 6, the main reaction's (k_3) activation energy is 16.05 kJ/mol, and the activation energy of the side reactions are − 62.59–59.94 kJ/mol. The presence of negative activation energy in it may be due to multi-step equilibrium reactions [37]. Compared with the main reaction, most of the side reactions' activation energies were relatively large, indicating that a low temperature favors the main reaction while a high temperature favors the side reactions. As the reaction temperature increased, the by-products would increase substantially, leading to a decrease in the quality of the alkylated oil, which was consistent with the pattern found in the single-factor experiments.

Conclusions

The CCD method in RSM was used to conduct a multi-factorial analysis of the C_4 alkylation reaction process to investigate the interactions between the reaction factors and then optimize the reaction conditions. The influence of the influencing factors on the selectivity of TMPs was investigated using the single-factor method, and the optimal range of values was determined. Based on the experiments designed by the CCD method, a quadratic model of the interaction between the factors was established and fitted well with $R^2 = 0.9958$, $P < 0.0001$. It was discovered that the reaction time had the greatest impact on the selectivity of TMPs, followed by the reaction temperature. The relative error between the model's experimental and predicted values was 0.98%, and the values were 77.47% and 76.72%, respectively. The fact that there is no significant difference between experimental and estimated values demonstrates the excellent reliability of the proposed quadratic model.

The kinetic model for the alkylation reaction of isobutane/2-butene using H_2SO_4 as the catalyst was developed based on the classical carbenium ion mechanism. Nonlinear least square in Matlab was used for the model to estimate the parameters, with the rate constants and 95% confidence intervals obtained being reasonable. Based

on the Arrhenius relationship, the activation energies and pre-exponential factors of the various reactions were determined. The research revealed that the main reaction's (k_3) activation energy was 16.03 kJ/mol, while the activation energies of the side reactions ranged from 3.42 to 59.94 kJ/mol. It was noteworthy that k_1 had an activation energy of − 62.59 kJ/mol, which was probably the result of a multi-step equilibrium reaction. The kinetic model could estimate the variation of critical components in alkylates with time, namely C_5, C_6, C_7, TMPs, DMHs, C_9 and C_m. The results indicated that the estimated values of the model were well-fitted and in excellent agreement with the empirical data, demonstrating that the kinetic model was plausible and could serve as guidance for designing and optimizing reactors in the alkylation industry..

Declarations

Conflict of interest The authors declare that they have no known competing financial interests or personal relationships that could have appeared to influence the work reported in this paper.

References

1. Xin Y, Hu Y, Li M, Chi K, Zhang S, Gao F, Jiang S, Wang Y, Ren C, Li G (2020) Isobutane alkylation catalyzed by H_2SO_4: effect of H_2SO_4 acid impurities on alkylate distribution. Energy Fuels 35(2):1664–1676
2. Singhal S, Agarwal S, Singh M, Rana S, Arora S, Singhal N (2019) Ionic liquids: green catalysts for alkene-isoalkane alkylation. J Mol Liq 285:299–313
3. Wang D, Zhang T, Yang Y, Tang S (2019) Simulation and design microreactor configured with micromixers to intensify the isobutane/1-butene alkylation process. J Taiwan Inst Chem Eng 98:53–62
4. Gan P, Tang S (2016) Research progress in ionic liquids catalyzed isobutane/butene alkylation. Chin J Chem Eng 24(11):1497–1504
5. Guzmán-Lucero D, Guzmán-Pantoja J, Velázquez HD, Likhanova NV, Bazaldua-Domínguez M, Vega-Paz A, Martínez-Palou R (2021) Isobutane/butene alkylation reaction using ionic liquids as catalysts. Toward Sustain Ind Mol Catal 515:111892
6. Li Q, Zhang R, Li Y, Meng X, Liu H, Wang X, Xu C, Dong H, Su Q, Zhang X (2022) Reaction behaviors and mechanism of isobutane/propene alkylation catalyzed by composite ionic liquid. Ind Eng Chem Res 61(25):8624–8633
7. Hommeltoft SI (2001) Isobutane alkylation: Recent developments and future perspectives. Appl Catal A: Gen 221(1–2):421–428
8. Wang H, Meng X, Zhao G, Zhang S (2017) Isobutane/butene alkylation catalyzed by ionic liquids: a more sustainable process for clean oil production. Green Chem 19(6):1462–1489
9. Tian Y, Mei S, Zhang LL, Chu GW, Sun B, Fisher AC, Luo Y, Zou HK (2022) Improved H_2SO_4-catalyzed alkylation reaction in a rotating packed bed reactor by adding additives. Can J Chem Eng 100(11):3395–3407
10. Velázquez HD, Likhanova N, Aljammal N, Verpoort F, Martínez-Palou R (2020) New insights into the progress on the isobutane/butene alkylation reaction and related processes for high-quality fuel production. Crit Rev Energy Fuels 34(12):15525–15556
11. Ershov MA, Savelenko VD, Makhova UA, Kapustin VM, Abdellatief TM, Karpov NV, Dutlov EV, Borisanov DV (2022) Perspective towards a gasoline-property-first approach exhibiting octane hyper-boosting based on isoolefinic hydrocarbons. Fuel 321:124016

12. Ershov M, Potanin D, Tarazanov S, Abdellatief TM, Kapustin V (2020) Blending characteristics of isooctene, MTBE, and TAME as gasoline components. Energy Fuels 34(3):2816–2823
13. Zheng W, Li D, Sun W, Zhao L (2018) Multi-scale modeling of isobutane alkylation with 2-butene using composite ionic liquids as catalyst. Chem Eng Sci 186:209–218
14. Li L, Zhang J, Wang K, Luo G (2016) Caprolactam as a new additive to enhance alkylation of isobutane and butene in H_2SO_4. Ind Eng Chem Res 55(50):12818–12824
15. HöPfl VB, Schachtl T, Liu Y, Lercher JA (2022) Pellet size-induced increase in catalyst stability and yield in zeolite-catalyzed 2-butene/isobutane alkylation. Ind Eng Chem Res 61(1):330–338
16. Fu K, Liu B, Chen X, Chen Z, Liang J, Zhang Z, Wang L (2022) Investigation of a complex reaction pathway network of isobutane/2-butene alkylation by CGC–FID and CGC-MS-DS. Molecules 27(20):6866
17. Kore R, Scurto AM, Shiflett MB (2020) Review of isobutane alkylation technology using ionic liquid-based catalysts—where do we stand? Ind Eng Chem Res 59(36):15811–15838
18. Greer AJ, Jacquemin J, Hardacre C (2020) Industrial applications of ionic liquids. Molecules 25(21):5207
19. Salah HB, Nancarrow P, Al-Othman A (2021) Ionic liquid-assisted refinery processes–A review and industrial perspective. Fuel 302:121195
20. Schmerling L (1946) The mechanism of the alkylation of paraffins. II. Alkylation of isobutane with propene, 1-butene and 2-butene. J Am Chem Soc 68(2):275–281
21. Mosby J, Albright LJ (1966) Alkylation of isobutane with 1-butene using sulfuric acid as catalyst at high rates of agitation. Ind Eng Chem Prod Res Dev 5(2):183–190
22. Li K, Eckert RE, Albright LF (1970) Alkylation of isobutane with light olefins using sulfuric acid. Operating variables affecting physical phenomena only. Ind Eng Chem Process Des Dev 9(3):434–440
23. Langley JR, Pike RW (1972) The kinetics of alkylation of isobutane with propylene. AIChE J 18(4):698–705
24. Kramer G (1965) Hydride transfer reactions in concentrated sulfuric acid. J Org Chem 30(8):2671–2673
25. Sun W, Shi Y, Chen J, Xi Z, Zhao L (2013) Alkylation kinetics of isobutane by C4 olefins using sulfuric acid as catalyst. Ind Eng Chem Res 52(44):15262–15269
26. Li L, Zhang J, Du C, Wang K, Luo G (2018) Kinetics study of sulfuric acid alkylation of isobutane and butene using a microstructured chemical system. Ind Eng Chem Res 58(3):1150–1158
27. Li L, Zhang J, Du C, Luo G (2019) Intensification of the sulfuric acid alkylation process with trifluoroacetic acid. AIChE J 65(1):113–119
28. Zhang H, Tang H, Xu J, Li Y, Yang Z, Liu R, Zhang S, Wang Y (2018) Enhancement of isobutane/butene alkylation by aromatic-compound additives in strong Brønsted acid. Fuel 231:224–233
29. Ilaiyaraja N, Likhith K, Babu GS, Khanum F (2015) Optimisation of extraction of bioactive compounds from Feronia limonia (wood apple) fruit using response surface methodology (RSM). Food Chem 173:348–354
30. Meziant L, Benchikh Y, Louaileche H (2014) Deployment of response surface methodology to optimize recovery of dark fresh fig (Ficus carica L., var. Azenjar) total phenolic compounds and antioxidant activity. Food Chem 162:277–282
31. Zheng W, Wang Z, Sun W, Zhao L, Qian F (2021) H_2SO_4-catalyzed isobutane alkylation under low temperatures promoted by long-alkyl-chain surfactant additives. AIChE J 67(10):e17349
32. Myers RH, Montgomery DC, Anderson-Cook CM (2016) Response surface methodology: process and product optimization using designed experiments. Wiley, Hoboken
33. Box GE, Wilson KB (1992) On the experimental attainment of optimum conditions. In: Kotz S, Johnson NL (eds) Breakthroughs in statistics: methodology distribution. Springer, New York
34. Aschauer S J, Jess A J I, Research E C (2012) Effective and intrinsic kinetics of the two-phase alkylation of i-paraffins with olefins using chloroaluminate ionic liquids as catalyst. Ind Eng Chem Res 51(50):16288–16298
35. Yucel I (2012) Atmospheric model applications. InTechopen, Rijeka
36. Lebedeva NV, Nese A, Sun FC, Matyjaszewski K, Sheiko SS (2012) Anti-Arrhenius cleavage of covalent bonds in bottlebrush macromolecules on substrate. P Natl Acad Sci 109(24):9276–9280
37. Liu Y, Wu G, Pang X, Hu R (2020) Kinetics study on alkylation of isobutane with deuterated 2-butene in composite ionic liquids. Chem Eng J 387:123407